

Laser infrared photothermal radiometric depth profilometry of steels and its potential in rail track evaluation

A. Mandelis*, M. Munidasa, L. Nicolaides

Photothermal and Optoelectronic Diagnostics Laboratories, Department of Mechanical and Industrial Engineering, University of Toronto and Materials and Manufacturing Ontario, 5 King's College Road, Toronto, Ont, Canada M5S 3G8

Abstract

Laser Infrared Photothermal Radiometry has been utilized for several thermal-wave inverse-problem NDE applications. These include depth profilometry of steels and rails and scanning tomography of sub-surface defects in steels. Further, a computational algorithm has been refined to address the ill-posedness of the thermal-wave inverse problem. As a result, depth profiles of case-hardened steels, railway track heads from the field, and machined sub-surface hole thermal-diffusivity images have been reconstructed successfully using this emerging NDT technology. © 1999 Elsevier Science Ltd. All rights reserved.

Keywords: NDT technology; Laser infrared photothermal radiometry; Thermal wave slice diffraction tomography

1. Introduction

Among modern-day NDE methodologies, thermal-wave detection [1] is a technique growing in importance due to its ability to monitor sub-surface structures and damage in materials, well beyond the optical penetration depth of illumination sources, i.e. below the range of optical imaging of opaque materials. This relatively new technology is developed as a complementary tool (in terms of depth probing ranges) to acoustic and ultrasonic NDE, but for entirely different geometries and more general classes of materials, process and manufacturing parameters. In photothermal methods a beam of energy, typically a laser, modulated at a certain frequency is focused onto the sample surface. The resulting periodic heat flow in the material is a diffusive process, producing a periodic temperature distribution which is called a *thermal-wave*. This is spatially heavily damped and has a modulation frequency (f)-dependent penetration depth μ (diffusion length) given by

$$\mu = \sqrt{\frac{\alpha}{\pi f}}, \quad (1)$$

where α is the thermal diffusivity. This frequency dependence has been utilized to obtain depth-selective information on thermal diffusivity by measuring the amplitude and the phase of the periodic surface temperature of the sample

under investigation. Owing to the heavily damped nature of thermal waves, this technique is most suitable for detecting shallow defects and inhomogeneities ranging from a few micrometers to a few millimetres. The surface temperature oscillation could be detected either in the back-scattering or in the transmission mode using a variety of sensor probes. In this work we used the infrared (IR) photothermal radiometric detection method to measure the surface temperature which relies on the detection of variations in the IR radiation emitted from the sample surface that is excited by an intensity-modulated laser. The main advantage of this detection method is its non-contact remote sensing nature. The amplitude and the phase of the thermal-wave signal carry information about any heat transport disruption or change below the surface, which must be interpreted with appropriate models, in order to yield reliable reconstructions of the spatially variant thermal diffusivity of the sample.

In this paper we describe two different modes of application in steels: (1) thermal diffusivity depth profiling of near-surface inhomogeneities and (2) tomographic imaging of sub-surface defects. These applications serve as an introduction to a novel thermal-wave non-destructive testing technology in the field of steel quality monitoring and rail-track evaluation.

2. Apparatus

A schematic diagram of the experimental apparatus is shown in Fig. 1. An Ar⁺ laser (514 nm) modulated by an

* Corresponding author. Tel.: + 1-416-978-5106; fax: + 1-416-978-5106.

E-mail address: mandelis@mie.utoronto.ca (A. Mandelis)

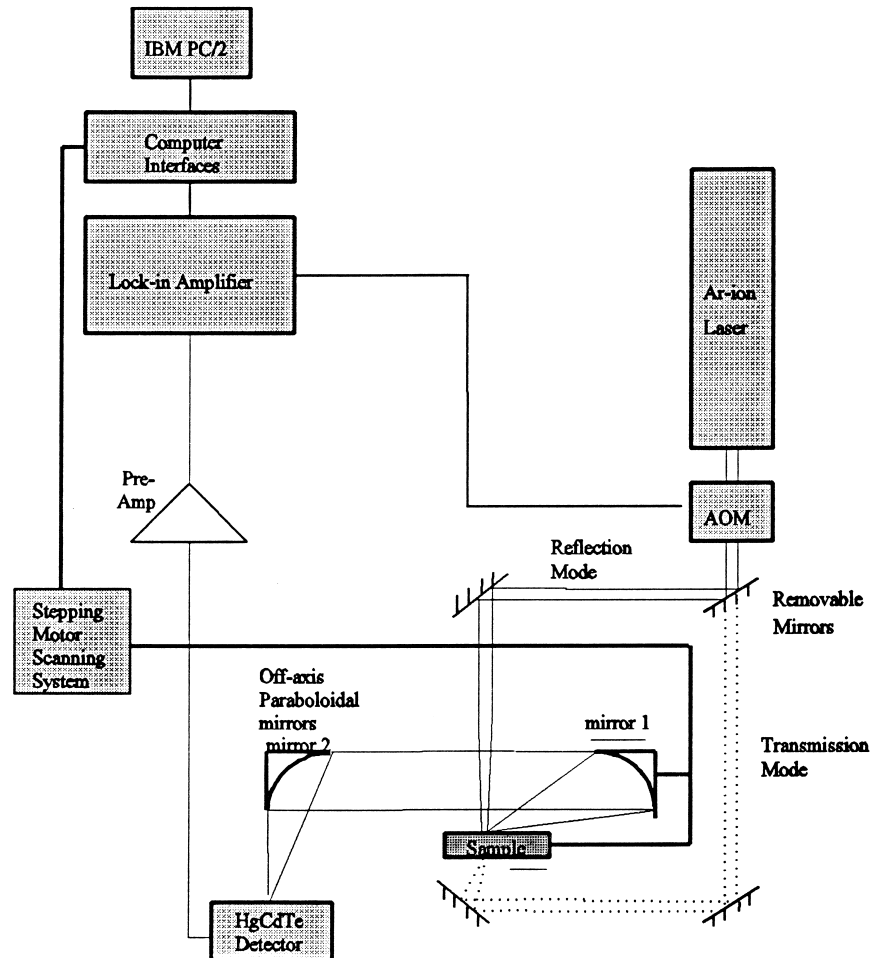


Fig. 1. Experimental apparatus.

acousto-optic modulator is directed onto the sample surface. The emitted IR radiation from the sample surface is collected and focused onto the detector using two off-axis paraboloidal mirrors [2]. The detector is a liquid N₂ cooled HgCdTe element with an active area of 1 mm² (50 μm² for imaging) and a spectrally selective range of 2–12 μm. A germanium window with a transmission bandwidth of 2–12 μm is mounted in front of the detector to block any visible radiation from the pump laser. For depth profiling, the pump beam spot size is made much larger than the maximum profiling depth, in order to maintain the one-dimensional heat diffusion formalism assumed in the theory. For tomographic imaging, the laser is focused to a 30 μm diameter spot. The detector signal is preamplified before being sent to a lock-in amplifier. For depth profile reconstruction, the lock-in amplifier outputs, amplitude and phase, are recorded at a range of laser modulation frequencies. For tomographic reconstruction, the spatial temperature profile is recorded along a line on the sample surface for a given laser position. This could be achieved by scanning the paraboloidal mirror at its focal position across a line on the surface of the sample. This is repeated for several laser positions on the same line. A detailed description of the

experimental procedure for each mode of application can be found elsewhere [3,4].

3. Depth profiling of steels

The thermal diffusivity, which depends on the microstructural properties of the material, is very sensitive to the changes that take place in the material as a result of surface modification processes such as laser processing, hardening and coating deposition. Considering this change in thermal diffusivity and the typical depths involved (a few micrometers to a few millimeters), photothermal techniques have proven to be reliable non-destructive and non-contact methods of profiling these subsurface inhomogeneities [3,5,6].

Photothermal phase and amplitude data obtained at a given location of a specimen may be inverted to reconstruct the thermal diffusivity depth profile at that location. In recent years several attempts have been made in inverting these data to reconstruct thermal diffusivity (conductivity) depth profiles, which are summarized in Ref. [7]. In this paper we will demonstrate the inversion methodology

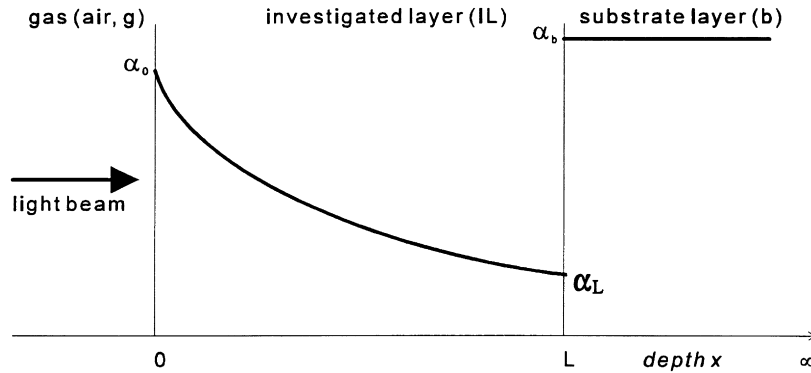


Fig. 2. An illustration of the relationship between depth versus thermal diffusivity for a test sample having an investigation layer of arbitrary thermal diffusivity profile, and a substrate layer.

based on the generalized theoretical formulation described in Refs. [7,8], in its applications to problems of concern to the steel industry, as a novel non-destructive evaluation technology.

Here we assume a steel layer of thickness L , with an exponential profile of the form

$$\alpha_s(x) = \alpha_0 \left(\frac{1 + \Delta e^{-qx}}{1 + \Delta} \right)^2, \quad (2)$$

where

$$\Delta = \frac{1 - \sqrt{\alpha_L/\alpha_0}}{\sqrt{\alpha_L/\alpha_0} - e^{-qL}}, \quad (3)$$

and α_0, α_L, q are constants representing the values of the thermal diffusivity at the two boundary surfaces ($x = 0, L$) of the material (Fig. 2), and the diffusivity gradient, respectively. The surface temperature response to the incident optical beam on the sample is normalized by the surface temperature response to the same beam, at the same

frequency, of a semi-infinite homogeneous material (a Zr alloy used as a reference). This gives for each frequency a data-pair, namely amplitude ratio and phase difference between sample and reference. The normalizing procedure is necessary for the correct accounting of all frequency dependencies in the apparatus other than that due to the investigated sample. Theoretical values of the data-pairs are calculated and are compared with the experimental values in estimating the local parameters α_L and q at each frequency using the numerical search algorithm described in Ref. [7].

The theoretical calculation is valid in principle for arbitrary exponential profiles $\alpha_s(x)$, wherein at every angular frequency ω_i the surface a.c. temperature response of a material structure gives two data channels, namely amplitude and phase. In practice, the validity of the calculated values is much more general than the assumed exponential profile of Eq. (2), as it is possible to update the fitted exponential profile at each experimental angular frequency ω_i through a new pair of values (α_0, q) or (α_L, q) . Here, the

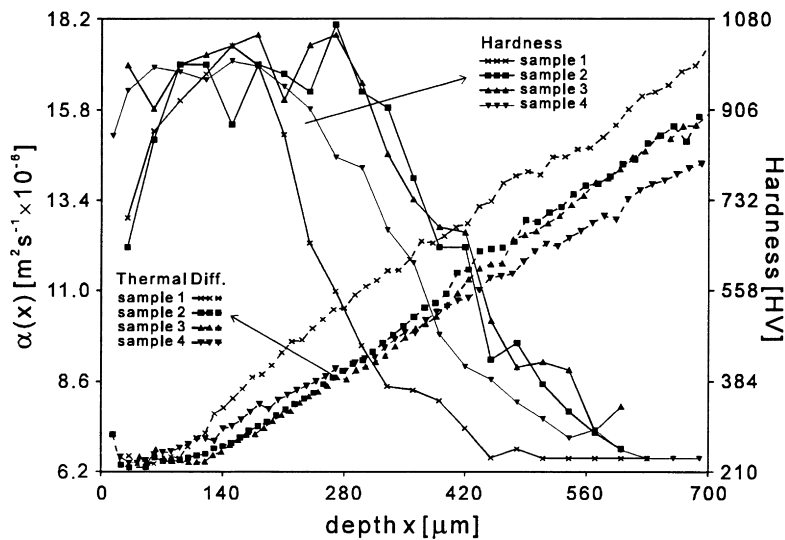


Fig. 3. Reconstructed thermal diffusivity profile of the case-hardened steel samples 1–4 down a depth of 700 μm . Microhardness measurements are also shown for comparison.

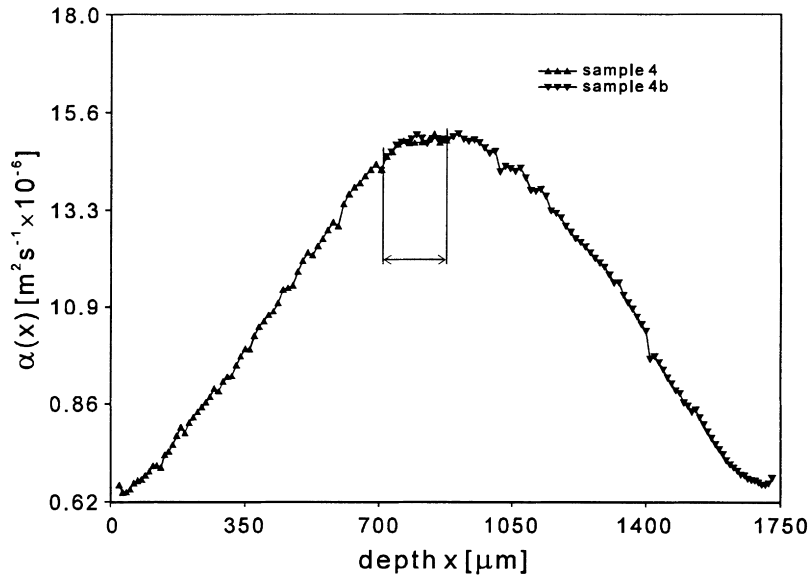


Fig. 4. Reconstructed depth profiles for the full depth range including the opposite side of sample No. 4 (designed as 4b).

thickness L and the thermal properties of the substrate are assumed to be known parameters. Thus entirely arbitrary depth profiles may be reconstructed by numerically determining the optimal pair of the foregoing values so that the sought profile locally results in the experimentally observed thermal-wave signal amplitude and phase data at each and every laser-beam-intensity modulation frequency.

3.1. Case hardened steel

We investigated four different case hardened steel samples made of C15 steel. The surface hardening of these samples has been achieved by dissolving additional carbon through the surface (carburization) and subsequent thermal treatment [9]. The thickness of the hardened layer

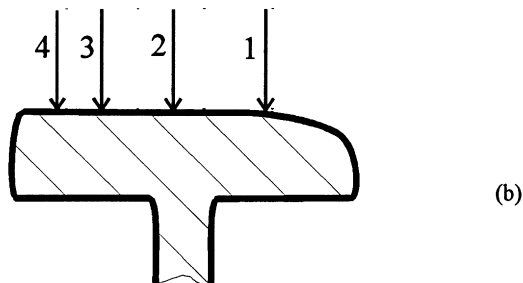
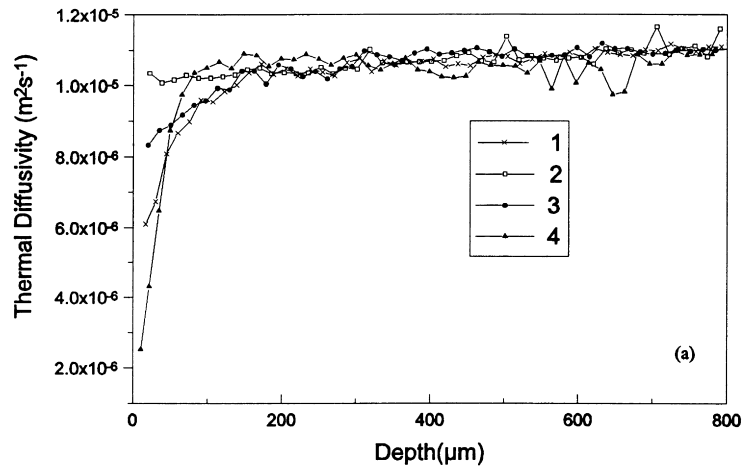


Fig. 5. (a) Thermal diffusivity depth profiles at four positions of the rail head as marked in (b).

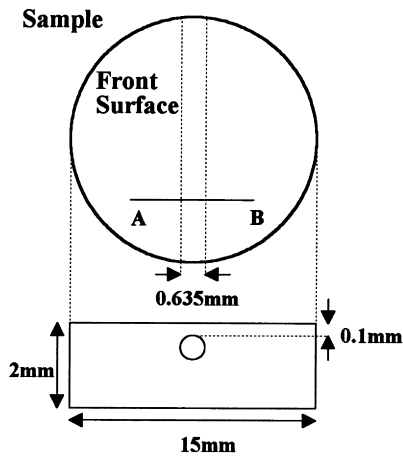


Fig. 6. Steel sample geometry with the hole used for tomographic scanning.

was varied by changing the carburization time from sample to sample. These samples could be treated theoretically as layers of thickness L on a homogeneous substrate (air). The resulting depth profiles down to a depth of $700\ \mu\text{m}$ for all four samples together with the available [6] microhardness profiles are shown in Fig. 3. These profiles show a close anti-correlation to hardness profiles including the upturn of the curve corresponding to sample no. 2 very near the surface. The surface roughness of the samples has been taken into account theoretically in reconstructing these profiles.

Although our diffusivity profiles do not show an identical inverse relation [6] to the hardness profiles, the variations from sample to sample (samples 1–3) are well correlated, as shown in Fig. 3. It should be noted here that the microhardness measurements were performed [6] not on the same sample but on a different set of samples, assumed to be identical. Reconstructed thermal diffusivity profiles of the case-hardened steel samples for the full depth range obtained from the data are shown in Fig. 4. The limiting factor that prohibited the profile to be obtained down to the other side of the samples from data taken from the opposite side was the three dimensional (lateral) heat flow that was not taken into account in the theory. This effect becomes significant at depths $\geq 1\ \text{mm}$ in the present samples. The obtained profiles clearly show that the diffusivity reaches a maximum around the middle of the sample and starts decreasing towards the opposite surface. The reconstructed profile from the opposite surface of one of the samples (sample 4) is also shown in Fig. 4 as sample 4b with its front surface at $1.75\ \text{mm}$, which is the thickness of this sample. It complements very well the profile from the opposite side forming a nearly symmetric diffusivity distribution, as expected from the identical exposure conditions of both surfaces to carburization. Further, in depth regions of overlap, the two profiles of sample 4 coincided well, as indicated by the double arrow in Fig. 4.

3.2. Railway track head

We have investigated a portion of railway track taken off the Toronto subway system for possible hardening of the rail head. The oxide was cleaned off the specimen using an emery paper. Investigations have shown that a thin layer of oxide could give faulty results. Four measurements were made along the width of the top surface as shown in Fig. 5. The reconstructed thermal diffusivity profiles show a lower diffusivity down to a depth of about $150\ \mu\text{m}$ throughout the width of the sample. In detail, the extent of the deterioration of the thermal parameter is maximum close to the cold work end of the rail and less around the curved end. The change is minimal in the mid portion. Unfortunately, at the moment, destructive hardness measurements are available only in the mid portion (from surface down to $5\ \text{mm}$) of the rail head; they show little change in hardness, as expected consistently with the thermal diffusivity profiles.

4. Tomographic imaging of sub-surface defects in steels

Thermal wave slice diffraction tomography (TSDT) is a photothermal imaging technique for NDE, leading to the detection and imaging of sub-surface cross-sectional defects in opaque solids in the very-near-surface region (μm – mm). The conventional reconstructions of the well-posed propagation wave-field tomographies cannot be applied in the case of the thermal wave problem. The differentiation of TSDT from the other tomographic technologies is partly based on the fact that the imaged quantity is the cross-sectional thermal diffusivity, instead of, for instance, the ultrasonic velocity. Unlike electromagnetic or acoustic tomography, thermal wave tomography suffers from the facts that: (a) propagation distances of the thermal wave are short; (b) the thermal wave vector is complex lying along the 45° line in the complex plane; and (c) the sample cannot be rotated in most practical situations with steel sheets or railway track heads. Therefore, the conventional reconstruction of the well-posed propagation wave-field tomographies cannot be applied in the case of the thermal wave problem. A theoretical/computational technique utilizing the Tikhonov regularization method to invert almost singular matrices resulting from the ill-posedness of the inverse thermal wave problem has been developed [10,11] for the reconstruction of thermal diffusivity cross-sectional images in materials. Experimentally the technique is made truly non-contact by obtaining cross-sectional scans of sub-surface defects through laser photothermal radiometric detection. The emitted blackbody radiation field resulting from a heating focused laser beam across a material cross-section is sampled, and the scanned photothermal radiometric signal is recorded in back-scatter or transmission at each relative laser position. The numerically reconstructed experimental data constitute a tomographic image

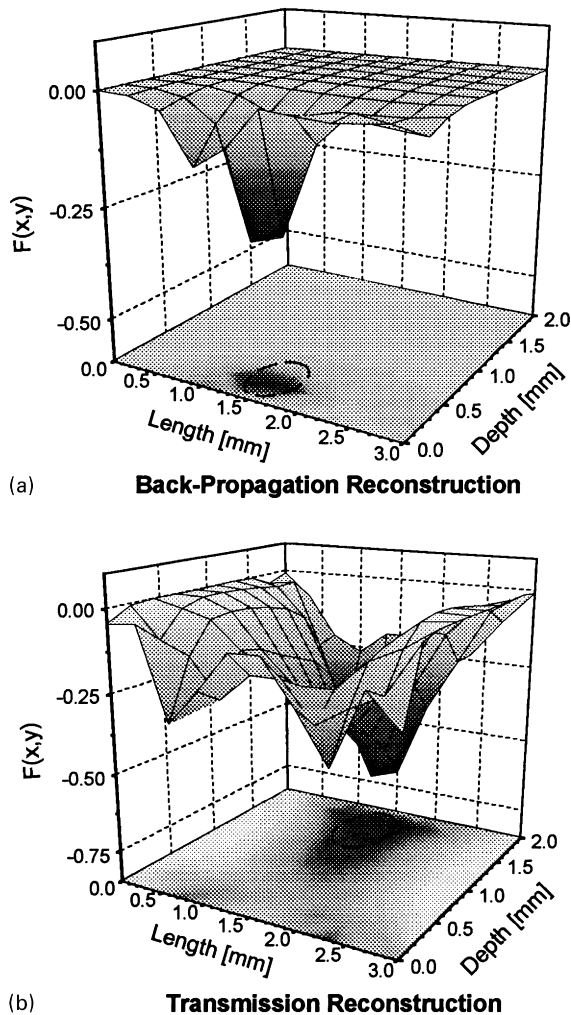


Fig. 7. (a) TSDT back-propagation reconstruction of shallow defect. (b) TSDT transmission reconstruction of deep defect. Both are average of five laser positions. True defect shown by dashed lines $F(x,y) = \alpha_{\text{steel}}/\alpha_{\text{defect}} - 1$.

of the cross-sectional thermal diffusivity across a plane perpendicular to the sample surface.

Fig. 6 shows a 2 mm-thick stainless steel test sample with a 0.6 mm-diameter shallow hole drilled parallel to the surface 0.1 mm below the surface. Data has been collected along the line AB and reconstructed to image the cross-section underneath. Fig. 7(a) is an average *back-propagation reconstruction* of five individual back-propagation reconstructions of the shallow defect (at five different laser positions). Fig. 7(b) is an average *transmission reconstruction* of five individual transmission reconstructions from a steel with a deeper sub-surface defect. Straight averaging of five laser position scans was found to be very efficient in producing a good reconstruction as any artifacts created by individual reconstructions were diminished. In Fig. 7 the dashed closed lines indicate the true position of the defects. When comparing the reconstruction quality of Fig. 7(a) and (b) it is observed that shallow defects image better in back-propagation, and deep defects image better in transmission.

Further, more precise information about the back of the defect is obtained in transmission than in back-propagation. In transmission mode the imaging of the front surface of the defect is less precise. Straight averaging of constructions of back-propagation and transmission scans lead to an optimal reconstruction of the defect.

5. Conclusions

In this paper we have described a novel, reliable non-destructive remote sensing technology which allows the reconstruction of thermal diffusivity profiles in inhomogeneous samples and steel in particular. The steel sample may be an inhomogeneous layer of finite thickness on a homogeneous substrate; a free standing layer, i.e. with air as the substrate; or a thick piece (*semi-infinite solid*) with its inhomogeneity continuously varying as a function of the depth coordinate. This technology shows strong potential for use as an evaluation method for steel plants and railway tracks. We have also demonstrated a tomographic imaging technique for off-line, near surface cross-sectional imaging of steels. The implications of the research, besides establishing rigorous theoretical/computational and experimental foundations of thermal-wave depth profilometric and tomographic technologies, are quite broad in that they have the potential to address ex situ and in situ quality control aspects of many manufacturing and field-level processes; the onset of deterioration of railway tracks, forming quantitative criteria for their maintenance and replacement cycles; and the presence of sub-surface damage (crack, fatigue) in industrial steels, for possible feedback and process yield enhancement of the manufactured product, or as failure prediction criteria in industrial structures.

Acknowledgements

The support of the Materials and Manufacturing Ontario (MMO) and the Natural Sciences and Engineering Research Council of Canada (NSERC) are gratefully acknowledged.

References

- [1] Progress in photothermal and photoacoustic science and technology. In: Mandelis A, editor. Nondestructive evaluation (NDE), II. Englewood Cliffs, NJ: Prentice-Hall, 1994.
- [2] Mandelis A, Munidasa M. Depth profilometry of near-surface inhomogeneities via laser-photothermal probing of the thermal diffusivity of condensed phases. *Int J Thermophys* 1994;15:1299–309.
- [3] Munidasa M, Ma T-C, Mandelis A, Brown SK, Mannik L. Non-destructive depth profiling of laser processed Zr-2.5 Nb alloy by infrared photothermal radiometry. *Mater Sci Engng* 1992;A159:111–8.
- [4] Nicolaidis L, Munidasa M, Mandelis A. Thermal-wave infrared radiometric slice diffraction tomography with back-propagation and transmission reconstructions: experimental. *Inverse Problems* 1997;13:1413–25.

- [5] Ma T-C, Munidasa M, Mandelis A. Photoacoustic frequency-domain depth profilometry of surface-layer inhomogeneities: application to laser processed steels. *J Appl Phys* 1992;71:6029–35.
- [6] Lan TTN, Seidel U, Walther HG, Goch G, Schmitz B. Experimental results of photothermal microstructural depth profiling. *J Appl Phys* 1995;78:4108–11.
- [7] Mandelis A, Funak F, Munidasa M. Generalized methodology for thermal diffusivity depth profile reconstruction in semi-infinite and finitely thick inhomogeneous solids. *J Appl Phys* 1996;80:5570–8.
- [8] Munidasa M, Funak F, Mandelis A. Application of a generalized methodology for quantitative thermal diffusivity depth profile reconstruction in manufactured inhomogeneous steel-based materials. *J Appl Phys* 1998;83:3495–8.
- [9] H.G. Walther's group, Friedrich-Schiller-Universität Jena, Jena, Germany.
- [10] Padé O, Mandelis A. Computational thermal-wave slice tomography with back-propagation and transmission reconstructions. *Rev Sci Instrum* 1993;64:3548–62.
- [11] Nicolaidis L, Mandelis A. Image-enhanced thermal-wave slice diffraction tomography with numerically simulated reconstruction. *Inverse Problems* 1997;13:1393–412.